



Published in final edited form as:

Pain. 2013 August ; 154(8): 1170–1180. doi:10.1016/j.pain.2013.02.027.

Knockdown of sodium channel Na_v1.6 blocks mechanical pain and abnormal bursting activity of afferent neurons in inflamed sensory ganglia

Wenrui Xie, Judith A. Strong, Ling Ye, Ju-Xian Mao, and Jun-Ming Zhang

Pain Research Center, Department of Anesthesiology, University of Cincinnati College of Medicine, 231 Albert Sabin Way, Cincinnati, OH, 45267, USA

Abstract

Inflammatory processes in the sensory ganglia contribute to many forms of chronic pain. We previously showed that local inflammation of the lumbar sensory ganglia rapidly leads to prolonged mechanical pain behaviors and high levels of spontaneous bursting activity in myelinated cells. Abnormal spontaneous activity of sensory neurons occurs early in many preclinical pain models, and initiates many other pathological changes, but its molecular basis is not well understood. The sodium channel isoform Na_v1.6 can underlie repetitive firing and excitatory persistent and resurgent currents. We used *in vivo* knockdown of this channel via local injection of siRNA to examine its role in chronic pain following local inflammation of the rat lumbar sensory ganglia. In normal DRG, quantitative PCR showed that cells capable of firing repetitively had significantly higher relative expression of Na_v1.6. In inflamed DRG, spontaneously active bursting cells expressed high levels of Na_v1.6' immunoreactivity. *In vivo* knockdown of Na_v1.6 locally in the lumbar DRG at the time of DRG inflammation completely blocked development of pain behaviors and abnormal spontaneous activity, while having only minor effects on unmyelinated C-cells. Current research on isoform-specific sodium channel blockers for chronic pain is largely focused on Na_v1.8, because it is present primarily in unmyelinated C fiber nociceptors, or on Na_v1.7, because lack of this channel causes congenital indifference to pain. However, the results suggest that Na_v1.6 may be a useful therapeutic target for chronic pain, and that some pain conditions may be primarily mediated by myelinated A-fiber sensory neurons.

Keywords

Nav1.6; Scn8a; back pain; spontaneous activity; allodynia; inflammation

Introduction

Abnormal spontaneous activity of sensory neurons is an early event in many different models of neuropathic or inflammatory pain [10,29,3]. This abnormal activity plays a key

© 2013 International Association for the Study of Pain. Published by Elsevier B.V. All rights reserved.

Corresponding author: Jun-Ming Zhang, M.D., M.Sc. Pain Research Center Department of Anesthesiology University of Cincinnati 231 Albert Sabin Way Cincinnati, OH 45267-0531 Phone 513-558-2427 Fax 513-558-0995 Jun-Ming.Zhang@uc.edu.

The authors declare no competing financial interests.

Publisher's Disclaimer: This is a PDF file of an unedited manuscript that has been accepted for publication. As a service to our customers we are providing this early version of the manuscript. The manuscript will undergo copyediting, typesetting, and review of the resulting proof before it is published in its final citable form. Please note that during the production process errors may be discovered which could affect the content, and all legal disclaimers that apply to the journal pertain.

role in initiating pain behaviors [4,21] as well as other pathological changes such as sympathetic sprouting onto sensory neurons [37,38] and glial activation [40]. Hence understanding the ionic basis of spontaneous activity may contribute to development of treatments for chronic pain conditions, which are common and difficult to treat with current therapies [12].

We previously described a model in which robust, long-lasting mechanical hypersensitivity is induced by local inflammation of the L5 dorsal root ganglion (DRG) in rats [41,36]. This model is most directly related to conditions such as chemogenic low back pain, in which local inflammation of the DRG may occur, but is also of general interest because direct effects of inflammatory mediators on sensory neurons play a role in many pain conditions and preclinical pain models, including neuropathic pain models [1,42]. Local inflammation of the DRG results in a rapid increase in spontaneous high-frequency bursting activity of cells with myelinated axons, as measured with microelectrode recordings in isolated whole DRG. This spontaneous activity and the underlying subthreshold membrane oscillations are sensitive to TTX and to riluzole, a drug that shows some selectivity for persistent Na currents. Riluzole applied locally to the inflamed DRG was effective in reducing mechanical pain if applied at the time of DRG inflammation [36].

DRG neurons express multiple isoforms of TTX-sensitive sodium channels. Most, including $Na_V1.6$, can mediate persistent currents, in addition to the much larger transient, fast-inactivating sodium currents that underlie the action potential. Persistent currents can contribute to the membrane potential oscillations that underlie spontaneous activity. $Na_V1.6$ can also give rise to a resurgent sodium current, a brief reopening observed near the resting potential following a depolarization (or action potential). Resurgent current facilitates high frequency repetitive and bursting firing [8], which is observed after DRG inflammation. Interestingly, a recent study using both human subjects and mice showed that the cooling – induced neuropathic pain induced by the chemotherapy drug oxaliplatin was mediated by enhancement of $Na_V1.6$ -mediated persistent and resurgent currents in myelinated sensory neurons [27]. Because TTX- and riluzole-sensitive high frequency bursting activity of myelinated sensory neurons plays a key role in the DRG inflammation pain model, we hypothesized that $Na_V1.6$ might play an important role in the pain behaviors and spontaneous activity observed after DRG inflammation. As there are few highly specific pharmacological tools to study this channel, we used local *in vivo* knockdown of $Na_V1.6$ in the lumbar DRG with siRNA. We report that knockdown of this channel completely blocks both reflexive indications of pain evoked by mechanical stimulation and abnormal spontaneous activity induced by DRG inflammation.

Materials and Methods

Surgical procedure for local inflammation of the DRG

The experimental protocol was approved by the Institutional Animal Care and Use Committee of the University of Cincinnati. Experiments adhered to the guidelines of the Committee for Research and Ethical Issues of IASP. Adult Sprague Dawley rats (Harlan, Indianapolis, USA) were used for all experiments. Male rats weighing 150 - 200 g at the start of the experiment (for behavior experiments) or females weighing 100 –150 grams at the time of sacrifice (for electrophysiological experiments) were used. Behavioral measurements in 100 – 120 gram female animals confirmed that the DRG inflammation induced mechanical hypersensitivity and effects of $Na_V1.6$ knockdown were similar to that observed in the larger males (see Results). The L5 DRG was inflamed by depositing the immune activator zymosan (2 mg/ml, 10 μ l, in incomplete Freund's adjuvant (IFA)) over the L5 DRG as previously described [36].

Procedure for in vivo injection of siRNA into the DRG

siRNA directed against rat Nav1.6 channel (gene ID 29710) and nontargeting control were designed by and purchased from Dharmacon/ThermoFisher (Lafayette, CO). Except where noted, experiments used siGENOME™ siRNA consisting of a “smartpool” of four different siRNA constructs combined into one reagent. Catalog numbers were M-094591-00 (directed against Nav1.6) and D-001210-02 (nontargeting control directed against firefly luciferase, screened to have minimal off-target effects and least 4 mismatches with all known human, mouse and rat genes according to the manufacturer). The sequences for the 4 constructs directed against Nav1.6 were: construct 1, CGACUGAGGUGGAAAUUAA; construct 2, CAACAUCGAGGAAGGACUA; construct 3, GCAUUAUUCGCCUUAUGA; construct 4, GAAAUCCGGUUCGAAAUUCG. 3 μL aliquots containing 80 pmoles of siRNA made up with cationic linear polyethylenimine (PEI)-based transfection reagent (“in vivo JetPEI”, Polyplus Transfection, distributed by WVR Scientific, USA) at a nitrogen/phosphorus ratio of 8 were injected into each L4 and L5 DRG on one side, through a small glass needle (75 μm o.d.) inserted close to the DRG through a small hole cut into the overlying membrane close to the site where the dorsal ramus exits the spinal nerve, as previously described [35]. We chose to inject siRNA into both L4 and L5 DRG because there may be some spread of the zymosan/IFA from L5 into L4, and because the hindpaw receives innervation from both L5 and L4.

Behavior testing

Mechanical sensitivity was tested by applying a series of von Frey filaments to the heel region of the paws, using the up-and-down method [7]. A cutoff value of 15 grams was assigned to animals that did not respond to the highest filament strength used. A wisp of cotton pulled up from, but still attached to a cotton swab was stroked mediolaterally across the plantar surface of the hindpaw to score the presence or absence of a brisk withdrawal response to a normally innocuous mechanical stimulus (light touch-evoked tactile allodynia). Thermal sensitivity of the hindpaw was measured using the Hargreaves method [13].

Electrophysiology

Intracellular recording in current clamp mode was performed at 36 – 37° C using microelectrodes on sensory neurons near the dorsal surface of an acutely isolated whole DRG preparation, as previously described [36]. This preparation allows neurons to be recorded without enzymatic dissociation, with the surrounding satellite glia cells and neighboring neurons intact [28,43]. The DRG was continuously perfused with ACSF (in mM: NaCl 130, KCl 3.5, NaH₂PO₄ 1.25, NaHCO₃ 24, Dextrose 10, MgCl₂ 1.2, CaCl₂ 1.2, 16 mM HEPES, pH = 7.3, bubbled with 95% O₂/ 5% CO₂). Cells were classified by conduction velocity (stimulation of attached dorsal root) as C-cells (unmyelinated) if the conduction velocity was <1.2 m/s; faster velocities were defined as A-cells (myelinated) [30]. Any spontaneous activity observed after impalement of the cell was recorded first, and re-confirmed at the end of the recording period. Input resistance and action potential (AP) parameters were measured with injected current steps of increasing size after adjusting the bridge balance circuit to compensate for the voltage drop across the electrode. AP threshold, width, and peak V were measured during the response to the smallest current that evoked an action potential (rheobase) during a 75 msec depolarization. The AP voltage threshold was defined as the first point on the rising phase of the spike at which the change in voltage exceeded 1/10th of the maximum value. Duration of the AP was measured at the threshold voltage. The cell was then given longer (270 msec) suprathreshold currents to determine the maximum number of AP that could be evoked. Rheobase for spontaneously active cells was defined as zero.

Immunostaining for Na_v1.6 in DRG sections and whole mount

DRG sections were cut at 10 μ m on a cryostat after fixation in 4% paraformaldehyde in 0.1M Phosphate Buffer and 4% sucrose. The polyclonal antibody against Na_v1.6 was from Alomone (Jerusalem, Israel; catalog ASC-009) used at 1:100 dilution. The antibody specificity was previously demonstrated by a lack of staining in a knockout mouse [5]. The secondary antibody conjugated to Alexa Fluor 594 (Invitrogen, Carlsbad, CA) was used at a dilution of 1:1000. Images from ~10 sections of each DRG were captured under a confocal microscope using Slidebook 4.1 imaging acquisition software (Intelligent Imaging Innovation, Denver, CO). To measure the expression of Na_v1.6 in the DRG neurons, the summed intensities of Na_v1.6 signal were measured and normalized by the cellular area in each analyzed section to give an intensity ratio. In all immunohistochemical experiments, data from at least three animals were included to control for interanimal variability. For experiments involving double staining for Na_v1.6 and the neuronal marker NeuN (mouse anti-NeuN, 1:1000, Abcam Cambridge, MA) or the myelination marker NF200 (mouse anti-hypophosphorylated neurofilament H (NF200) 1:100, Abcam), the procedure was the same except that sequential incubations with the two primary antibodies and two secondary antibodies were conducted using the same incubation parameters.

For immunostaining in whole mount DRG preparations of Na_v1.6 in neurons identified as spontaneously active or firing only single APs, then injected with biocytin during recording, the whole DRG was fixed at the end of the recording session for up to 2 hours in 4% paraformaldehyde in 0.1 M Phosphate Buffer and 4% sucrose followed by antigen retrieval in trypsin working solution. After incubation in Na_v1.6 antibody and secondary antibody, multiple layers of biocytin labeled neurons from the surface of whole DRG were captured under a confocal microscope.

Quantitative PCR

To test for siRNA-induced changes in cytokines IFIT1 and of IFN γ , cDNA was synthesized from whole DRGs (3 days after siRNA treatment or untreated controls). Quantitative real time -PCR (qPCR) was performed on the MPx3005 instrument (Stratagene, Santa Clara, CA) and analyzed as previously described [31]. Briefly, the baseline, PCR efficiency and threshold cycle were calculated using LinRegPCR analysis software [25]. Significance of relative expression differences was determined with the REST-2008 program (Version 2.0.7) [22] which incorporates correction for amplification efficiencies (as determined by LinReg). Expression data was normalized to expression of hypoxanthine phosphoribosyltransferase 1 (HPRT) which was determined to be the most stable reference gene amongst 4 tested in 23 DRG samples, as indicated by the BestKeeper program [23] and not altered by DRG inflammation [31]. All primers were designed using Primer-BLAST software (www.ncbi.nlm.nih.gov/tools/primer-blast/) [24]. Primer sequences were: IFIT1 (RNA reference XM_220058.3), TCTCCAGCACCATGAGTGAAGAA (forward), TTGCCCCAGGTCACCAGGCT (reverse). IFN γ (RNA reference NM_138880.2), ACGCCGCGTCTTGTTTTGC (forward), GGTGTTCACCTCGAACTTGGCG (reverse). HPRT (RNA reference NM_012583): GCAGACTTTGCTTTCCTTGG (forward), TACTGGCCACATCAACAGGA (reverse).

Similar analysis methods were used to compare Na_v1.6 and Na_v1.7 expression in cells identified as capable of firing only a single action potential, or bursts of multiple action potentials, in response to injected current. For these experiments, the cDNA was synthesized from cytoplasm samples isolated from 5 – 10 cells injected during recording with Alexa Fluor 488 or 594 hydrazide. At the end of the recording session, the DRG was incubated in 10 ml collagenase (0.5% in ACSF) for 15 min and then cytoplasm samples were collected. The contents of the labeled cells were sucked into a glass pipette (25 to 30 μ m tip diameter)

under microscopic observation which confirmed that surrounding glial cells were excluded. Samples were processed to cDNA using the Superscript III CellsDirect Synthesis System (Invitrogen) according to the manufacturer's instructions, a process that included DNA digestion and reverse transcription using poly dT primers. All primers were designed to anneal at 60°C, to avoid regions of the sodium channels which have strong homology to other sodium channels, and to amplify across an exon boundary to avoid contamination from genomic DNA. Primer sequences used were: Nav1.6 (RNA reference, NM_019266.2) : TACAGTGGCTACAGCGGCTA (forward), TGTTTGTGACCACGCTCATT (reverse). Nav1.7 (RNA reference NM_133289): GACAGCTTCTCCAGAGGTGATAATA (forward), CCATGGTGGACATTTTTGTCT (reverse).

Data analysis

Comparison of values between different experimental groups was done using nonparametric methods for data that did not show a normal distribution based on the D'Agostino and Pearson omnibus normality test. The statistical test used in each case is indicated in the text, or figure or table legend. Significance was ascribed for $p < 0.05$. Levels of significance are indicated by the number of symbols, e.g., *, $p = 0.01$ to < 0.05 ; **, $p = 0.001$ to 0.01 ; ***, $p < 0.001$. Data are presented as average \pm S.E.M.

Results

Nav1.6 knockdown in normal animals reduces repetitive firing evoked by intracellular current injection and does not affect cutaneous sensitivity to mechanical stimulation

We first investigated the distribution of Nav1.6 in normal, noninflamed lumbar DRG stained with an antibody whose specificity was previously demonstrated by a lack of staining in a knockout mouse [5]. Consistent with previous reports [5,11], many DRG neuron somas expressed Nav1.6, including cells positive for NF200, a marker of myelinated cells [18], and (generally smaller diameter) cells negative for NF200 (Fig. 1). However, the very largest cells were less likely to be Nav1.6 positive. Although overall 39% of cells in normal DRG were Nav1.6 positive, a subset of cells was much more intensely stained. These tended to be cells in the medium diameter range.

Knockdown of Nav1.6 after local DRG injection of Nav1.6 siRNA into normal, non-inflamed DRG was verified using immunocytochemistry 3 days later. The relative density of Nav1.6 immunostaining was reduced over 2-fold, from 21062 ± 618 to 9423 ± 1397 intensity units/ μm^2 ($p = 0.002$, t-test) compared to control animals that received nontargeting siRNA. An example is shown in Fig.1G-I.

Because Nav1.6 has previously been shown to play a role in allowing repetitive firing, we next determined whether its expression was higher in sensory neurons capable of firing repetitively in a bursting pattern in response to suprathreshold current injections. cDNA was synthesized from cytoplasm collected from cells identified during microelectrode recording as capable of firing repetitively, or capable of firing only a single action potential. For these experiments, much stronger current stimulation was used than in other experiments, in order to ensure that cells firing single action potentials were incapable of multiple firing even with strong stimulation. Quantitative real-time PCR was used to amplify Nav1.6 and Nav1.7 Na channels from these samples, along with the reference gene V1.6 but not HPRT. Cells capable of repetitive firing had significantly higher relative expression of Nav1.6 but not Nav1.7 (Fig. 2A).

The mechanical threshold (von Frey test) was not affected by Nav1.6 knockdown on either the ipsilateral side (Fig. 2D) or the contralateral side. The thermal threshold (Hargreaves test) was also unaffected by siRNA treatment: the ipsilateral withdrawal latency in Nav1.6

siRNA treated animals ($n = 7$) was 10.9 ± 0.2 prior to surgery, 9.9 ± 0.2 two days after siRNA treatment. For nontargeting siRNA treated animals ($n = 6$) the latency was 10.7 ± 0.2 prior to surgery and 9.4 ± 0.6 two days after. None of the differences between groups or time points was significant (2-way RM ANOVA with Bonferroni posttests). Contralateral thermal withdrawal latencies were not significantly different from ipsilateral.

The electrophysiological effects of injecting siRNA directed against the $\text{Na}_V1.6$ channel into the L4/L5 DRG were investigated in normal DRGs using sharp-microelectrode recording in isolated whole DRG preparations. Recordings were made 3 days after siRNA injection. For analysis, cells were divided into C-cells (presumed unmyelinated) and A-cells (presumed myelinated), based on conduction velocity measured by electrical stimulation of the dorsal root. The primary electrophysiological effects of $\text{Na}_V1.6$ knockdown were a significant reduction in the percentage of A-cells capable of firing multiple (>2) action potentials (Fig. 2E), and in the number of action potentials A-cells were capable of firing in response to suprathreshold 270 msec current injections of 1 nA to 4 nA (Fig. 2F). Data on additional electrophysiological parameters is shown in Table 1. Several parameters were unaffected by $\text{Na}_V1.6$ knockdown. However, in A-cells treated with $\text{Na}_V1.6$ siRNA, the conduction velocity was significantly lower; and the rheobase was significantly higher, increasing from 1.2 ± 0.1 nA to 1.6 ± 0.1 ($p = 0.0008$, Mann-Whitney test).

$\text{Na}_V1.6$ is upregulated after DRG inflammation and preferentially expressed in bursting cells

$\text{Na}_V1.6$ expression was upregulated on postoperative day (POD) 3 by immunohistochemistry measurements (Fig. 3A). After DRG inflammation a higher percentage of cells expressed $\text{Na}_V1.6$ ($p < 0.001$, Chi square test; Fig. 3B, C). This increase occurred across the entire range of cell diameters although the largest cells still seemed less likely to show intense staining (see example in Fig. 5C). In separate experiments comparing the size distribution of cells in fixed sections with that in live cells as visualized in the whole DRG preparation used for recording, we determined that considerable shrinkage occurred during fixation. The peak of the size distribution in live cells was around 40 – 45 μm , compared to ~25 μm in fixed tissue.

To determine whether $\text{Na}_V1.6$ was more highly expressed in cells with spontaneous bursting after DRG inflammation, cells identified as spontaneously bursting or as firing only a single AP in response to strong current injection were injected with biocytin after recording (Fig. 4). The DRG was then fixed and stained for $\text{Na}_V1.6$ in a whole-mount preparation. Most bursting cells, but no single AP cells, were strongly $\text{Na}_V1.6$ -positive (Fig. 4D; $p < 0.001$, Chi-Square test).

$\text{Na}_V1.6$ knockdown blocks behavioral and electrophysiological effects of DRG inflammation

Next, we examined the effects of $\text{Na}_V1.6$ knockdown in L4/L5 DRG on mechanical hypersensitivity induced by local inflammation of the DRG. We have previously shown that DRG inflammation leads to a rapid (within 1 day) and long-lasting (>30 days) ipsilateral mechanical hypersensitivity[36]. When nontargeting control siRNA was injected into the DRGs at the time of DRG inflammation, the mechanical hypersensitivity had a similar time course and magnitude to that previously reported in the absence of siRNA (Fig. 5). However, when siRNA against $\text{Na}_V1.6$ was injected, the ipsilateral mechanical hypersensitivity induced by DRG inflammation was completely blocked for the entire 30 day observation period (Fig. 5A). Mechanical allodynia as measured by the cotton wisp test was also blocked by $\text{Na}_V1.6$ siRNA (Fig. 5B). As shown previously, contralateral effects of DRG inflammation measured with the von Frey method were minor and reached

significance only on POD 1 and 21 in the in the nontargeting siRNA injected group; the average threshold observed on these 2 days was 11.6 gram. No significant contralateral effects were observed in the Nav1.6 siRNA injected group. No responses to the cotton wisp test were observed on the contralateral side in either group. Thermal sensitivity was previously shown to be relatively unaffected by this model and so was not tested in these experiments. As in the uninflamed DRG, knockdown of Nav1.6 was confirmed by immunostaining (Fig.5C, D): intensity of Nav1.6 staining was reduced from 18374 ± 1794 intensity units/ μm^2 in nontargeting siRNA treated animals to 4630 ± 1608 intensity units/ μm^2 in Nav1.6 siRNA treated animals ($p = 0.0007$, t-test).

Most behavioral experiments including the von Frey testing shown in Figs 2 and 5 were done using male animals weighing 150 -200 grams, while electrophysiological experiments were done in younger, female animals which were found to have less connective tissue, facilitating the microelectrode impalements. In order to ensure that the electrophysiological experiments were relevant to the behavioral observations, we did behavioral measurements in some young female animals up to POD3, the time point at which they were sacrificed for electrophysiological experiments. The mechanical hypersensitivity was essentially identical between older males and younger females, and the same effects of DRG inflammation and Nav1.6 siRNA were observed: For Nav1.6 siRNA injected animals, the von Frey threshold on POD3 was 12.4 ± 1.0 grams in males ($n = 10$) compared to 14.7 ± 0.25 in young females ($n = 3$). For nontargeting siRNA injected animals, the values were 0.98 ± 0.23 in males ($n = 8$) compared to 0.86 ± 0.14 in young females ($N = 5$). A similar lack of sex differences was observed on POD1 (data not shown). None of the differences between males and young females was significant at any time point (2-way RM ANOVAs with Bonferroni posttests).

Previously we have shown that DRG inflammation results in a large increase in spontaneous activity in myelinated cells at POD3 [36]. In DRG injected with nontargeting siRNA at the time of DRG inflammation, a marked increase in the incidence of spontaneous activity of myelinated cells to 35% on POD3 was observed (Fig. 6), not significantly different from that previously observed after DRG inflammation in the absence of any siRNA (40%; $p = 0.3$, Fishers exact test). Most (89%) of the spontaneously active cells fired in a bursting pattern. In contrast, when DRG were treated with Nav1.6 siRNA at the time of inflammation, the incidence of spontaneous activity on POD3 was reduced to a level (6.2%) not significantly different from that seen in normal, uninflamed DRG injected with nontargeting siRNA (6.7%; Table 1), and not significantly different from the previously published value in normal DRG in the absence of any siRNA (4.8%; $p = 0.6$, Fishers exact test). As shown in Fig. 6, Nav1.6 siRNA also significantly reduced the fraction of A-cells capable of firing multiple action potentials, and the number of action potentials fired in non-spontaneously active cells in response to depolarizing current injections. In inflamed DRG, A-cells were also significantly hyperpolarized after Nav1.6 siRNA treatment, and several other parameters were significantly different from those cells treated with nontargeting siRNA, consistent with this hyperpolarization (threshold and maximum dV/dt ; Table 1). Parameters in C-cells were less affected by Nav1.6 siRNA, however, in C cells both the membrane potential and the AP threshold were ~ 4 mV more hyperpolarized, compared to C cells treated with nontargeting siRNA (Table 1).

The marked increase in spontaneous activity seen in myelinated cells on POD began to resolve by POD 7 – 10, at which time it was 14%, still significantly higher than in normal DRG ($p=0.014$), but significantly lower than on POD 3 ($p<0.001$; Fisher's exact test).

Evidence that behavioral effects of Nav1.6 knockdown are not due to off-target effects

The sequences of the 4 siRNA constructs that were pooled in the above knockdown experiments, like most commercially available siRNA constructs, were designed to be

specific for the $\text{Na}_v1.6$ gene; in particular, examination of the individual 19-base pair sequences showed no overlap greater than 10 base pairs with any other DRG Na_v channel sequences. However, there are several potential off-target mechanisms by which siRNA can generate a phenotype not directly related to knockdown of the target gene. One method is by nonspecific effects of the transfection method; however, the data presented compared transfection with a nontargeting siRNA to anti- $\text{Na}_v1.6$ siRNA, so nonspecific effects of the transfection reagent cannot account for the observed strong effects on behavioral sensitivity and electrophysiological properties. In addition, the behavioral and electrophysiological data from non-targeting siRNA treated animals were not significantly different from our previously published data in animals receiving no siRNA injections, indicating a lack of transfection reagent effects. A second off-target mechanism is the induction of the cellular immune response by the siRNA; there is some sequence dependence of this effect so the non-targeting control does not completely eliminate this possibility. Consideration of this effect is complicated by the fact that the model used here itself results in a large scale upregulation of many immune related genes [31]. Indeed, activation of the cellular immune response in the DRG would be more likely to result in increased hypersensitivity, not reduced. However, qPCR experiments comparing normal (non-inflamed) DRG treated with $\text{Na}_v1.6$ siRNA (isolated 3 days after siRNA injection) to untreated DRG found no significant upregulation of the message for the cytokine IFIT1, which has been proposed to be the best marker of the siRNA-induced cellular immune response [16]. We also found no significant upregulation by $\text{Na}_v1.6$ siRNA of mRNA for another cytokine that plays an important role in the cellular immune response, $\text{IFN}\gamma$. Finally, off-target effects may occur due to the siRNA binding in the 3' untranslated region of mRNA from non-targeted genes and inhibiting translation by acting similarly to endogenous regulatory micro RNAs. Such effects are concentration and sequence dependent, but unfortunately it is not yet possible to predict such effects from bioinformatics or to choose sequences that show no potentially problematic overlap with the 3' UTR of any other gene. To address this possibility we adopted the approach of Jackson and Linsley [16]. The $\text{Na}_v1.6$ siRNA that was so effective in blocking mechanical pain after DRG inflammation consisted of a pool of 4 siRNAs. We determined whether at least some of the individual constructs contained in this pool were also effective in blocking hypersensitivity after DRG inflammation. While not every individual member of the pool of 4 will necessarily provide effective knockdown of the target gene, at least some should provide knockdown while avoiding any sequence-specific off-target effects of the other three members of the pool. Before testing individual constructs we determined that the concentration used was close to the minimum required; this is desirable since the above off-target effects are concentration dependent. We found that injecting 1/10 th as much anti- $\text{Na}_v1.6$ siRNA gave a less complete block of the mechanical hypersensitivity induced by DRG inflammation (Fig. 7B). Next, 3 of the 4 individual constructs were tested. The total amount of siRNA injected was the same as in the experiments using pooled siRNA, i.e., 4 times the concentration of an individual construct was present in the individual injections as in the smart-pool injection. Two different constructs (#1 and #2) gave a behavioral phenotype (measured on POD3) not significantly different from that observed using the pooled construct, suggesting that the behavioral phenotype could not be attributed to off-target effects. A third construct (#4) had a significantly smaller effect in ameliorating the mechanical hypersensitivity (Fig. 7A). It was observed during both the dilution experiments and the testing of individual constructs that the behavioral data was noisier than observed with the pooled construct – individual animals showed either very large or very small behavioral effects. If the behavioral effects of the anti- $\text{Na}_v1.6$ siRNA are due to specific knockdown of the target gene, then in individual animals the amount of knockdown as indicated by staining with the anti $\text{Na}_v1.6$ antibody should correlate with the behavioral sensitivity of that animal. (Note that none of the individual siRNA constructs was directed at the region of the channel used to generate the antigen). This correlation was indeed observed: on POD3-4, the behavioral sensitivity of

individual animals was significantly and negatively correlated ($r=-0.72$, $p = 0.0008$, Spearman's correlation test) with the degree of knockdown as measured by immunohistochemistry in DRG sections from the same animals (Fig. 7). Taken together these results suggest that block of inflammation-induced hypersensitivity by the $\text{Na}_v1.6$ siRNA smartpool construct is not due to off-target effects.

Discussion

We found that knocking down $\text{Na}_v1.6$ locally within the dorsal root ganglion had profound effects in blocking both mechanical pain, and the abnormal spontaneous activity in myelinated neurons that are induced by DRG inflammation. The pain model used in this study, local inflammation of the lumbar DRG, rapidly induces a long-lasting and very pronounced increase in mechanical sensitivity of the paw. Mechanical pain measures were completely restored to normal values by treating with $\text{Na}_v1.6$ siRNA at the time of DRG inflammation. At the same time, the marked increase in spontaneous activity in myelinated neurons observed in inflamed DRG was also completely normalized. These findings are consistent with our previous studies in several different pain models showing that various manipulations designed to reduce or block the early period of abnormal spontaneous activity will also reduce pain behaviors for many weeks or months (the duration of the experiment). However, the results presented here are the most complete reversal of pain behaviors that we have observed with any manipulation. For example, in our previous study using this model, local perfusion of the DRG with riluzole significantly reduced mechanical hypersensitivity, but at some time points the effect was incomplete. In earlier studies, blocking nerve activity at the injury site in two different neuropathic pain models starting 10 days after injury [39] or perfusing the inflamed DRG with riluzole starting 1 week after injury (preliminary studies from our lab) was not effective in permanently reducing mechanical sensitivity. In addition, the initial high incidence of spontaneous activity in this (see Results) and other models [39] is not maintained for the duration of the mechanical hypersensitivity. We interpret this to mean that an early period of spontaneous activity is able to initiate long-lasting pain behaviors, but at later times maintenance of the pain behaviors does not depend on spontaneous activity in the DRG. This probably accounts for the prolonged effect of $\text{Na}_v1.6$ siRNA treatment on behavior observed here, as it seems unlikely that a single siRNA treatment would knock down the channel for a month. Indeed our preliminary observations suggest that significant recovery of $\text{Na}_v1.6$ staining occurs by 7 days.

We chose to investigate the effects of $\text{Na}_v1.6$ knockdown in this pain model because this channel can mediate persistent Na currents and, unlike most isoforms normally present in the DRG, resurgent currents [9]. Both of these currents could play a role in the observed spontaneous activity induced by DRG inflammation, the persistent current by providing a depolarizing contribution to the observed membrane potential oscillations, and the resurgent current by allowing high frequency repetitive firing [19,8]. The loss of spontaneous activity after $\text{Na}_v1.6$ knockdown is consistent with this previous literature though our data do not indicate the relative importance of effects on persistent, resurgent, or transient currents. Though $\text{Na}_v1.6$ can mediate persistent and resurgent currents, these currents are not present in every cell expressing $\text{Na}_v1.6$; additional cell-specific factors that are not completely understood also come into play in determining the ratio of transient to persistent or resurgent currents. Resurgent and persistent currents share many common regulators, including the $\text{Na}_v\beta4$ subunit [2], several drugs [32], and an epilepsy model [14]. Pharmacological separation of persistent and resurgent currents may prove difficult, but if blocking abnormal spontaneous activity is to be considered a therapeutic target, agents that block both may be quite useful.

Nav1.6 knockdown somewhat surprisingly led to significant hyperpolarization of the resting membrane potential in both A- and C-cells (Table I). This was only observed in inflamed DRG on POD3. One possible explanation is that the hyperpolarization was due to loss of Nav1.6-mediated persistent current, and that persistent currents make a significantly greater contribution to the resting potential after inflammation. Consistent with this, inflammation per se caused a significant 4 mV depolarization of A-cells in control (nontargeting-injected) DRG although for C cells the depolarization did not reach significance (2.4 mV; $p = 0.19$). A greater contribution of persistent current to the resting potential in inflamed DRG could reflect the general upregulation of Nav1.6 (Fig. 3A), and/or a specific increase in the persistent current contributed per channel. An increase in persistent current was reported in a related back pain model, chronic compression of the DRG [34].

The lack of marked effects of Nav1.6 knockdown on most electrical parameters of C cells (other than resting potential) was also surprising, given that many small-diameter and NF200-negative cells showed staining for Nav1.6. One possibility is that this may be due to the high expression of Nav1.8 in C cells, which may dominate some of the action potential properties measured, especially since the resting potential is more positive than in A cells. Alternatively, the Nav1.6 channel in C cells as viewed with immunohistochemistry may not be in an active or membrane form in the soma. Another possible explanation is that the antibody is staining a different protein; however, the loss of staining in siRNA treated cells argues against this (the antibody and siRNA would have to have coincidentally overlapping nonspecific effects), as does the previous validation of this antibody in a knockout mouse[5].

The Nav1.6 channel is the primary channel in nodes of Ranvier of peripheral nerve, and is also distributed along axons of C-fibers. Yet we found no change in mechanical or thermal sensitivity for 3 days following Nav1.6 knockdown. The von Frey method we used is not designed to measure increases in mechanical threshold as most animals already reach the cutoff value. It may be that reducing channel density in the more remote axons requires a more prolonged treatment due to the time required to affect proteins that must undergo axonal transport. In addition, the peripheral node has a high safety factor; the time course for lethality in different Nav1.6 knockouts suggests that the critical threshold for survival is 1 – 2% of normal levels [20]. Presence of Nav1.6 in the DRG cell bodies of various diameters, (including unmyelinated cells), as observed here, has been previously reported[17,5,11].

Nav1.6 has been shown to accumulate proximal to the injury site in a pain model involving constriction of the infraorbital nerve [15]. It has been implicated in a preclinical model of chemotherapy-induced pain [27], which, like the model used here, does not involve axon transection. However, because of the widespread distribution of Nav1.6 in both CNS and PNS, and because of its key role in the peripheral node, this channel has been generally discounted as a good therapeutic target for chronic pain. Instead, much work is focused on Nav1.8 because of its enrichment in nociceptors (however, this has recently been called into question[26]) and on Nav1.7 because its loss in humans creates congenital insensitivity to pain. We propose that it may be premature to eliminate Nav1.6 as a therapeutic target. Some pain models including the one used here seem to be based on abnormal activity in cells with myelinated axons that are not C-cells and may not even be nociceptors. In preliminary experiments we have observed that knockdown of Nav1.7 has no effect on mechanical sensitivity in this model. In addition, it may prove feasible to preferentially target abnormal spontaneous activity while sparing normal nerve transmission, with either use-dependent blockers or drugs which more selectively target persistent and/or resurgent currents. Such drugs have been previously described (see Introduction and [32]) though their selectivity is not ideal. In addition, developing drugs that penetrate the CNS poorly should be quite feasible; often the problem lies in getting drugs into the brain. In conclusion, this study

suggests that $\text{Na}_v1.6$ may play a key role in some chronic pain conditions, particularly those that do not involve axon transection.

Although $\text{Na}_v1.6$ is prominently expressed in DRG neurons and fibers (Fig. 1), it is also expressed in (and has functional effects in) some nonneuronal cells including macrophages[6]. Macrophages resident in the DRG may play important roles in some chronic pain models [33], and siRNA applied as in our experiments should have been available to both neurons and nonneuronal cells. This represents another route by which $\text{Na}_v1.6$ knockdown may have had behavioral and electrophysiological effects in our experiments.

Acknowledgments

Supported by NIH grants NS55860 and NS45594 (J-M Z.). We thank Dr. Mark Baccei for helpful comments on the manuscript

References

- [1]. Austin PJ, Moalem-Taylor G. The neuro-immune balance in neuropathic pain: involvement of inflammatory immune cells, immune-like glial cells and cytokines. *J Neuroimmunol.* 2010; 229:26–50. [PubMed: 20870295]
- [2]. Bant JS, Raman IM. Control of transient, resurgent, and persistent current by open-channel block by Na channel beta4 in cultured cerebellar granule neurons. *Proc Natl Acad Sci U S A.* 2010; 107:12357–12362. [PubMed: 20566860]
- [3]. Bedi SS, Yang Q, Crook RJ, Du J, Wu Z, Fishman HM, Grill RJ, Carlton SM, Walters ET. Chronic spontaneous activity generated in the somata of primary nociceptors is associated with pain-related behavior after spinal cord injury. *J Neurosci.* 2010; 30:14870–14882. [PubMed: 21048146]
- [4]. Berger JV, Knaepen L, Janssen SP, Jaken RJ, Marcus MA, Joosten EA, Deumens R. Cellular and molecular insights into neuropathy-induced pain hypersensitivity for mechanism-based treatment approaches. *Brain Res Rev.* 2011; 67:282–310. [PubMed: 21440003]
- [5]. Black JA, Renganathan M, Waxman SG. Sodium channel $\text{Na}(v)1.6$ is expressed along nonmyelinated axons and it contributes to conduction. *Brain Res Mol Brain Res.* 2002; 105:19–28. [PubMed: 12399104]
- [6]. Carrithers MD, Chatterjee G, Carrithers LM, Offoha R, Iheagwara U, Rahner C, Graham M, Waxman SG. Regulation of podosome formation in macrophages by a splice variant of the sodium channel SCN8A . *J Biol Chem.* 2009; 284:8114–8126. [PubMed: 19136557]
- [7]. Chaplan SR, Bach FW, Pogrel JW, Chung JM, Yaksh TL. Quantitative assessment of tactile allodynia in the rat paw. *Journal of Neuroscience Methods.* 1994; 53:55–63. [PubMed: 7990513]
- [8]. Cruz JS, Silva DF, Ribeiro LA, Araujo IG, Magalhaes N, Medeiros A, Freitas C, Araujo IC, Oliveira FA. Resurgent Na^+ current: a new avenue to neuronal excitability control. *Life Sci.* 2011; 89:564–569. [PubMed: 21683085]
- [9]. Cummins TR, Dib-Hajj SD, Herzog RI, Waxman SG. $\text{Nav}1.6$ channels generate resurgent sodium currents in spinal sensory neurons. *FEBS Lett.* 2005; 579:2166–2170. [PubMed: 15811336]
- [10]. Devor M. Ectopic discharge in Abeta afferents as a source of neuropathic pain. *Exp Brain Res.* 2009; 196:115–128. [PubMed: 19242687]
- [11]. Dib-Hajj SD, Cummins TR, Black JA, Waxman SG. Sodium channels in normal and pathological pain. *Annu Rev Neurosci.* 2010; 33:325–347. [PubMed: 20367448]
- [12]. Finnerup NB, Sindrup SH, Jensen TS. The evidence for pharmacological treatment of neuropathic pain. *Pain.* 2010; 150:573–581. [PubMed: 20705215]
- [13]. Hargreaves K, Dubner R, Brown F, Flores C, Joris J. A new and sensitive method for measuring thermal nociception in cutaneous hyperalgesia. *Pain.* 1988; 32:77–88. [PubMed: 3340425]

- [14]. Hargus NJ, Merrick EC, Nigam A, Kalmar CL, Baheti AR, Bertram EH 3rd, Patel MK. Temporal lobe epilepsy induces intrinsic alterations in Na channel gating in layer II medial entorhinal cortex neurons. *Neurobiol Dis.* 2011; 41:361–376. [PubMed: 20946956]
- [15]. Henry MA, Freking AR, Johnson LR, Levinson SR. Sodium channel Nav1.6 accumulates at the site of infraorbital nerve injury. *BMCNeurosci.* 2007; 8:56.
- [16]. Jackson AL, Linsley PS. Recognizing and avoiding siRNA off-target effects for target identification and therapeutic application. *Nat Rev Drug Discov.* 2010; 9:57–67. [PubMed: 20043028]
- [17]. Krzemien DM, Schaller KL, Levinson SR, Caldwell JH. Immunolocalization of sodium channel isoform NaCh6 in the nervous system. *J Comp Neurol.* 2000; 420:70–83. [PubMed: 10745220]
- [18]. Lawson SN, Waddell PJ. Soma neurofilament immunoreactivity is related to cell size and fibre conduction velocity in rat primary sensory neurons. *J Physiol.* 1991; 435:41–63. [PubMed: 1770443]
- [19]. Magistretti J, Castelli L, Forti L, D'Angelo E. Kinetic and functional analysis of transient, persistent and resurgent sodium currents in rat cerebellar granule cells in situ: an electrophysiological and modelling study. *J Physiol.* 2006; 573:83–106. [PubMed: 16527854]
- [20]. Meisler MH, Kearney J, Escayg A, MacDonald BT, Sprunger LK. Sodium channels and neurological disease: insights from Scn8a mutations in the mouse. *Neuroscientist.* 2001; 7:136–145. [PubMed: 11496924]
- [21]. Nieto FR, Cobos EJ, Tejada MA, Sanchez-Fernandez C, Gonzalez-Cano R, Cendan CM. Tetrodotoxin (TTX) as a therapeutic agent for pain. *Mar Drugs.* 2012; 10:281–305. [PubMed: 22412801]
- [22]. Pfaffl MW, Horgan GW, Dempfle L. Relative expression software tool (REST) for group-wise comparison and statistical analysis of relative expression results in real-time PCR. *Nucleic Acids Res.* 2002; 30:e36. [PubMed: 11972351]
- [23]. Pfaffl MW, Tichopad A, Prgomet C, Neuvians TP. Determination of stable housekeeping genes, differentially regulated target genes and sample integrity: BestKeeper--Excel-based tool using pair-wise correlations. *Biotechnol Lett.* 2004; 26:509–515. [PubMed: 15127793]
- [24]. Rozen S, Skaletsky H. Primer3 on the WWW for general users and for biologist programmers. *Methods Mol Biol.* 2000; 132:365–386. [PubMed: 10547847]
- [25]. Ruijter JM, Ramakers C, Hoogaars WM, Karlen Y, Bakker O, van den Hoff MJ, Moorman AF. Amplification efficiency: linking baseline and bias in the analysis of quantitative PCR data. *Nucleic Acids Res.* 2009; 37:e45. [PubMed: 19237396]
- [26]. Shields SD, Ahn HS, Yang Y, Han C, Seal RP, Wood JN, Waxman SG, Dib-Hajj SD. Na(v)1.8 expression is not restricted to nociceptors in mouse peripheral nervous system. *Pain.* 2012
- [27]. Sittl R, Lampert A, Huth T, Schuy ET, Link AS, Fleckenstein J, Alzheimer C, Grafe P, Carr RW. Anticancer drug oxaliplatin induces acute cooling-aggravated neuropathy via sodium channel subtype Nav1.6-resurgent and persistent current. *Proc Natl Acad Sci U S A.* 2012; 109:6704–6709. [PubMed: 22493249]
- [28]. Song XJ, Hu SJ, Greenquist KW, Zhang J-M, LaMotte RH. Mechanical and thermal hyperalgesia and ectopic neuronal discharge after chronic compression of dorsal root ganglia. *Journal of Neurophysiology.* 1999; 82:3347–3358. [PubMed: 10601466]
- [29]. Sorkin LS, Yaksh TL. Behavioral models of pain states evoked by physical injury to the peripheral nerve. *Neurotherapeutics.* 2009; 6:609–619. [PubMed: 19789066]
- [30]. Stebbing MJ, Eschenfelder S, Habler HJ, Acosta MC, Janig W, McLachlan EM. Changes in the action potential in sensory neurones after peripheral axotomy in vivo. *Neuroreport.* 1999; 10:201–206. [PubMed: 10203309]
- [31]. Strong JA, Xie W, Coyle DE, Zhang JM. Microarray analysis of rat sensory ganglia after local inflammation implicates novel cytokines in pain. *PLoS One.* 2012; 7:e40779. [PubMed: 22815815]
- [32]. Theile JW, Cummins TR. Inhibition of Navbeta4 peptide-mediated resurgent sodium currents in Nav1.7 channels by carbamazepine, riluzole, and anandamide. *Mol Pharmacol.* 2011; 80:724–734. [PubMed: 21788423]

- [33]. Vega-Avelaira D, Geranton SM, Fitzgerald M. Differential regulation of immune responses and macrophage/neuron interactions in the dorsal root ganglion in young and adult rats following nerve injury. *Mol Pain*. 2009; 5:70. [PubMed: 20003309]
- [34]. Xie RG, Zheng DW, Xing JL, Zhang XJ, Song Y, Xie YB, Kuang F, Dong H, You SW, Xu H, Hu SJ. Blockade of persistent sodium currents contributes to the riluzole-induced inhibition of spontaneous activity and oscillations in injured DRG neurons. *PLoS One*. 2011; 6:e18681. [PubMed: 21541342]
- [35]. Xie W, Strong JA, Kays J, Nicol GD, Zhang JM. Knockdown of the sphingosine-1-phosphate receptor S1PR1 reduces pain behaviors induced by local inflammation of the rat sensory ganglion. *Neurosci Lett*. 2012; 515:61–65. [PubMed: 22445889]
- [36]. Xie W, Strong JA, Kim D, Shahrestani S, Zhang JM. Bursting activity in myelinated sensory neurons plays a key role in pain behavior induced by localized inflammation of the rat sensory ganglion. *Neuroscience*. 2012; 206:212–223. [PubMed: 22265726]
- [37]. Xie W, Strong JA, Li H, Zhang J-M. Sympathetic sprouting near sensory neurons after nerve injury occurs preferentially on spontaneously active cells and is reduced by early nerve block. *J Neurophysiol*. 2007; 97:492–502. [PubMed: 17065247]
- [38]. Xie W, Strong JA, Mao J, Zhang JM. Highly localized interactions between sensory neurons and sprouting sympathetic fibers observed in a transgenic tyrosine hydroxylase reporter mouse. *Mol Pain*. 2011; 7:53. [PubMed: 21794129]
- [39]. Xie W, Strong JA, Meij JT, Zhang J-M, Yu L. Neuropathic pain: Early spontaneous afferent activity is the trigger. *Pain*. 2005; 116:243–256. [PubMed: 15964687]
- [40]. Xie W, Strong JA, Zhang JM. Early blockade of injured primary sensory afferents reduces glial cell activation in two rat neuropathic pain models. *Neuroscience*. 2009; 160:847–857. [PubMed: 19303429]
- [41]. Xie WR, Deng H, Li H, Bowen TL, Strong JA, Zhang J-M. Robust increase of cutaneous sensitivity, cytokine production and sympathetic sprouting in rats with localized inflammatory irritation of the spinal ganglia. *Neuroscience*. 2006; 142:809–822. [PubMed: 16887276]
- [42]. Xu Q, Yaksh TL. A brief comparison of the pathophysiology of inflammatory versus neuropathic pain. *Curr Opin Anaesthesiol*. 2011; 24:400–407. [PubMed: 21659872]
- [43]. Zhang J-M, Song XJ, LaMotte RH. Enhanced excitability of sensory neurons in rats with cutaneous hyperalgesia produced by chronic compression of the dorsal root ganglion. *Journal of Neurophysiology*. 1999; 82:3359–3366. [PubMed: 10601467]

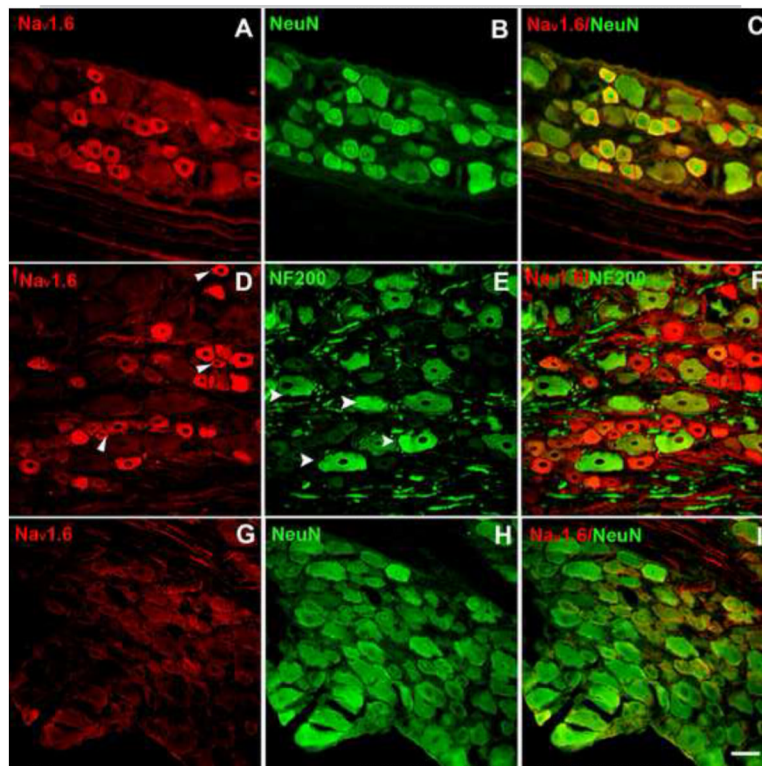


Figure 1. Examples of immunohistochemical staining of $\text{Nav}1.6$ in normal DRG sections. $\text{Nav}1.6$ signal is shown in red. Top: $\text{Nav}1.6$ (A), neuronal marker NeuN (green) (B), merged (C). Middle: $\text{Nav}1.6$ (D), arrowheads show examples of $\text{Nav}1.6$ positive, NF200 negative cells. NF200, marker for cells with myelinated axons (green) (E), arrowheads show example of NF200 positive, $\text{Nav}1.6$ negative cells. Merged (F). G-I, DRG sections 3 days after in vivo $\text{Nav}1.6$ siRNA treatment. Scale bar=50 μm .

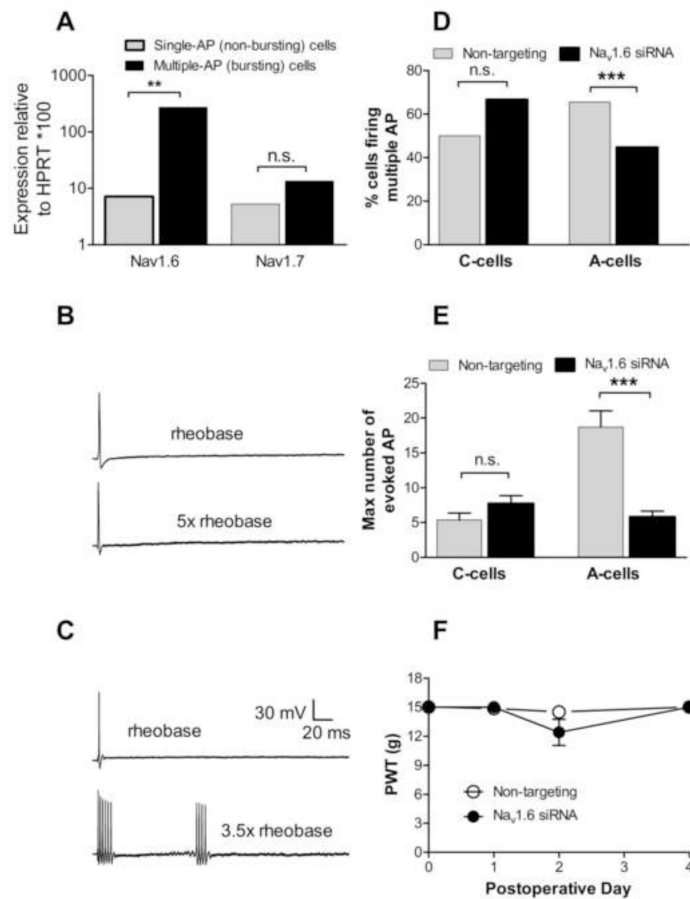


Figure 2.

Role of $\text{Na}_v1.6$ in normal DRG. A: cDNA synthesized from cytoplasm collected from cells identified by microelectrode recording as firing only a single action potential in response to incremental suprathreshold current injections (example shown in B) or capable of firing bursts of multiple action potentials (example shown in C). $N = 5$ samples for bursting cells, 12 samples for single AP cells. Each sample contained cytoplasm from 5 – 10 cells. Relative expression of $\text{Na}_v1.6$ (normalized to reference gene HPRT) but not of $\text{Na}_v1.7$ was significantly higher in cells capable of bursting. B and C: examples of voltage responses to current pulse injections in each cell type. For each example, the responses to the rheobase current and to the indicated suprathreshold current are shown. D, E: microelectrode recordings in DRG isolated 3 days after the siRNA treatments showed a decrease in the percentage of cells capable of firing >2 action potentials in response to injected current in A-cells (D); and in the maximum number of AP that could be evoked in non SA cells (E). For N values see Table 1. n.s., not significant; *, significant difference for the indicated comparison. In this and subsequent figures the level of significance is indicated by the number of symbols. F: paw withdrawal threshold (PWT) to mechanical stimuli (von Frey test) was not significantly affected by treating the L4 and L5 DRG with $\text{Na}_v1.6$ siRNA ($n = 9$) or nontargeting control siRNA ($n = 7$) on POD0. Baseline sensitivity (plotted as POD0) is average of 2 – 3 measurements on days prior to the surgery.

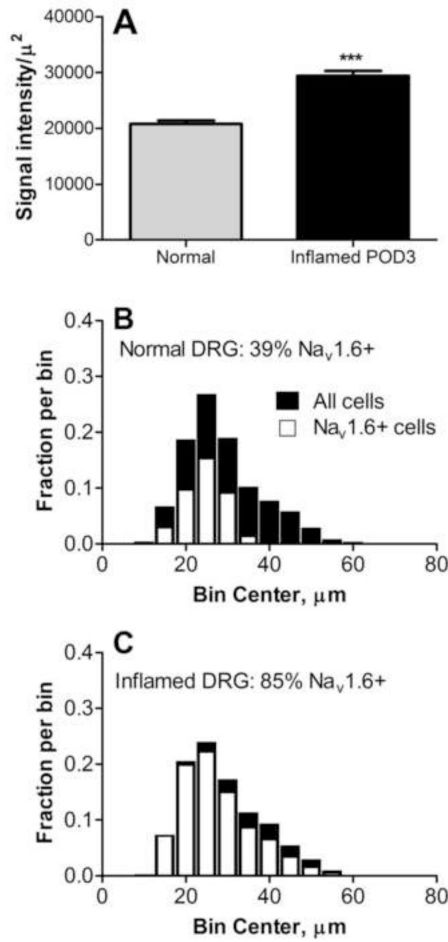


Figure 3. Na_v1.6 in inflamed DRG. A, Intensity of Na_v1.6 staining was higher in DRG sections from inflamed (POD3; n = 144 sections) than in normal DRG (n = 155 sections; Mann-Whitney test). B, C: size distribution of Na_v1.6 positive (white) and all (black) neurons in normal and inflamed DRG. N=6000-6500 cells per group. The distributions for the Na_v1.6 positive cells were scaled by the overall fraction of Na_v1.6 positive neurons. The scoring included lightly stained cells as well as more intensely stained cells.

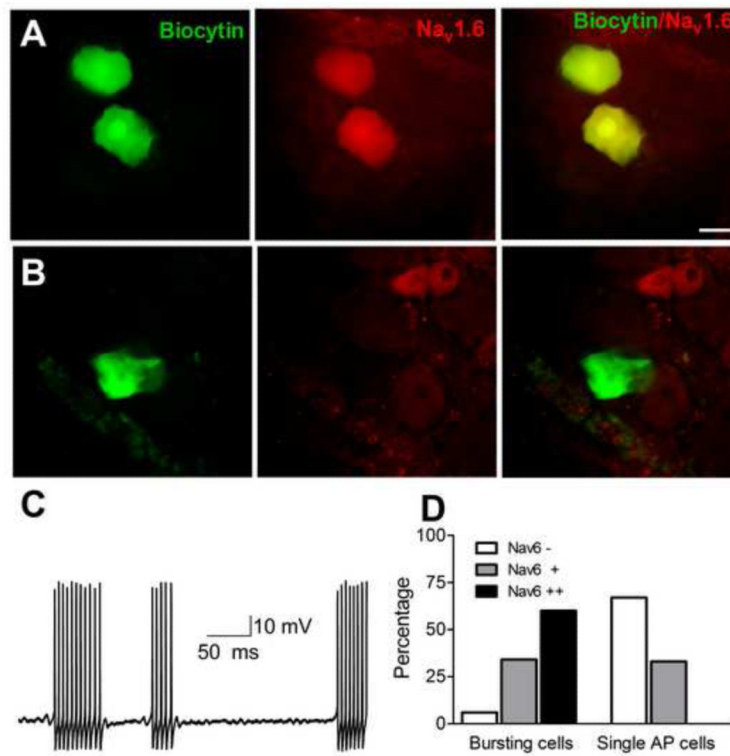


Figure 4.

: Bursting cells in inflamed DRG express higher levels of Nav_v1.6. A, example of 2 cells identified as spontaneously active during microelectrode recording that were injected with biocytin. After fixation, staining for Nav_v1.6 was done in whole mount DRG. B, example of biocytin injected cell that fired only a single AP in response to current injection. C: example of spontaneous activity recorded in an A-cell from a DRG treated with nontargeting siRNA and inflamed 3 days prior to recording. Note subthreshold oscillations between bursts of action potentials. D: summary data from 62 biocytin injected bursting cells and 36 biocytin injected single AP cells. Cells were scored as Nav_v1.6 negative(-), positive (+), or strongly positive (++) . Scale bar = 30 μ m.

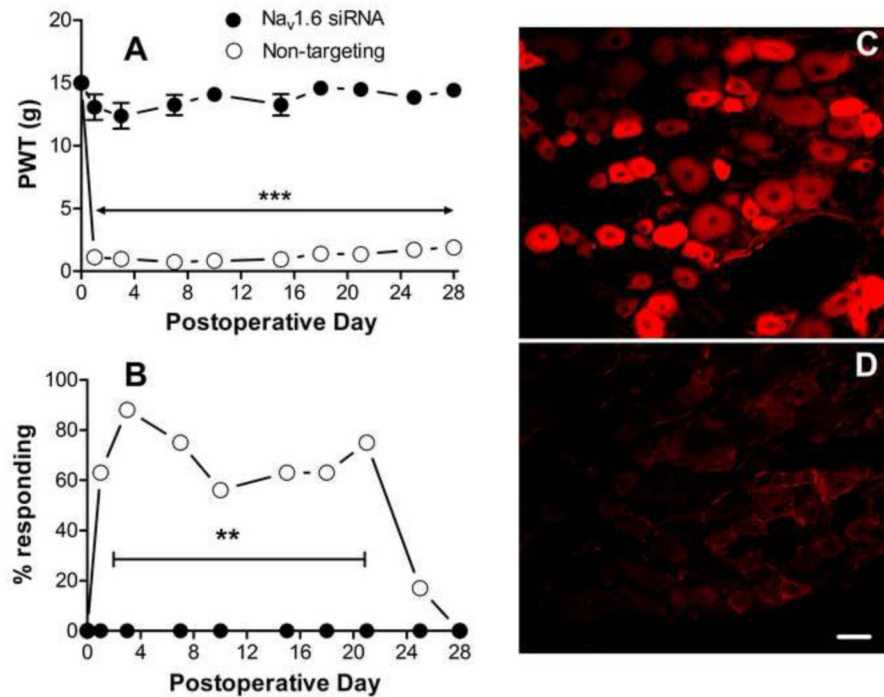


Figure 5. Effects of Nav_v1.6 knockdown after DRG inflammation. Nav_v1.6 siRNA or nontargeting siRNA was injected into the DRG at the time of DRG inflammation (POD0). Baseline values for ipsilateral paw withdrawal thresholds to mechanical stimuli (A) and the percent of animals withdrawing the paw in response to light stroking with a cotton wisp (B) were measured on 2 – 3 different days prior to surgery and the averages are plotted on POD0. A: prolonged mechanical hypersensitivity was observed in nontargeting siRNA treated animals (n = 8). This was completely abrogated in Nav_v1.6 siRNA injected animals (n = 10). ***, difference between the 2 groups was significant (p<0.001) on each POD (except baseline), 2-way RM ANOVA with Bonferroni posttest). B: percent responding to cotton wisp test. No animals responded prior to DRG inflammation on POD0. **, significant difference between groups on POD1 to POD 21, p<0.01 (except POD 3, p<0.001; and POD10, p<0.05), Fisher's exact test. C, D: examples of DRG sections from nontargeting (C) or Nav_v1.6 siRNA (D) treated inflamed DRG on POD3 stained for Nav_v1.6. Scale bar=50 μm.

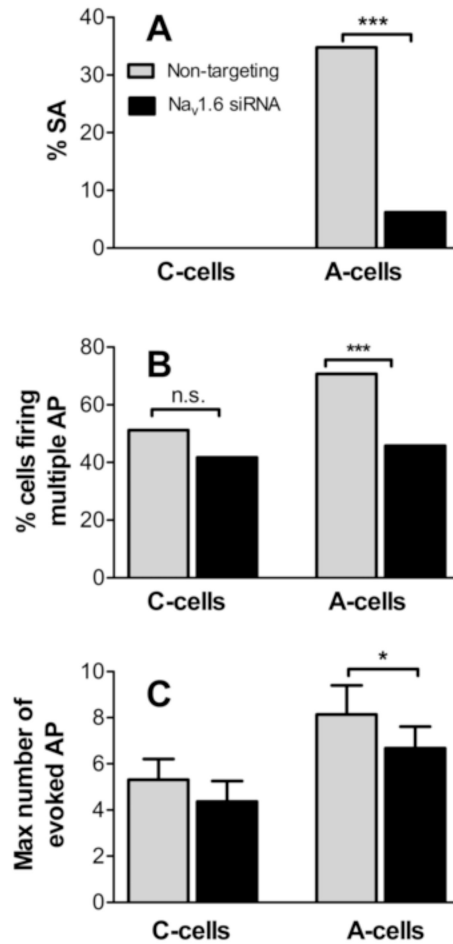


Figure 6. Electrophysiological effects of Nav_v1.6 knockdown in inflamed DRG measured on POD3. A, incidence of spontaneous activity (SA) measured was significantly reduced in A cells from Nav_v1.6 siRNA treated (Fisher's exact test). Incidence was zero in both C-cell groups. B, percent of cells capable of firing >2 AP in response to suprathreshold current injection (includes all SA cells). C, Maximum number of AP fired during 270 msec current injections (non SA cells only). For N values see Table 1.

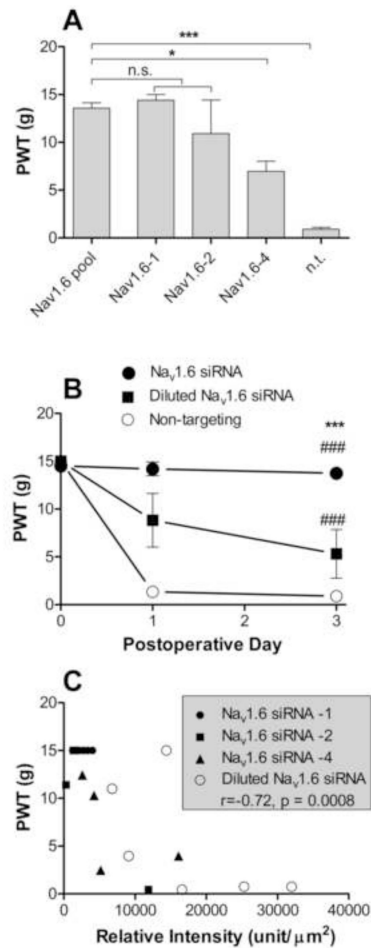


Figure 7.

Tests for off-target effects of the Nav_v1.6 siRNA. A, mechanical sensitivity 3 days after DRG inflammation and injection of a smartpool construct containing 4 different anti-Nav_v1.6 sequences (same as used in all previous experiments, data as in previous figures), or containing the same total siRNA amount of individual constructs number 1, 2, or 4 (N = 4 per group). Constructs 1 and 2, but not 4, gave similar amelioration of inflammation induced hypersensitivity. The hypersensitivity in nontargeting (n.t.) siRNA treated control animals is also replotted for reference. B, time course of mechanical sensitivity in animals injected with 1/10th the amount of smartpool siRNA as used in all other experiments (N = 6). C Behavioral data from individual animals from the experiments in parts A and B plotted against average Nav_v1.6 intensity measured in DRG sections from that animal on the same day (POD3-4). The values for correlation (r) and corresponding p value are from Spearman's correlation test

Table 1

Effects of Nav1.6 siRNA on electrophysiological parameters

	N	% SA	% firing multiple AP ^a	% with infected AP ^b	c.v. (m/s)	Maximum dV/dt (V/sec)	AP threshold (mV)	AP width (msec)	Maximum V during AP (mV)	Rheobase (nA)	Rheobase (non SA only)	Vrest (mV)	% with subthreshold oscillations ^c	Maximum # AP fired (not SA cells only)	
A cells: Normal DRG															
siRNA n.t.	165	6.7%	65.5%	18.2%	26.0 ± 1.4	396.9 ± 7.3	-53.4 ± 0.7	0.75 ± 0.03	25.4 ± 0.8	1.2 ± 0.1	1.3 ± 0.1	-66.6 ± 0.5	28.5%	18.7 ± 2.3	
siRNA Nav1.6	165	3.6%	44.8% ***	24.8%	16.9 ± 0.6 ***	390.2 ± 7.8	-53.3 ± 0.6	0.83 ± 0.03 **	25.4 ± 0.7	1.6 ± 0.1 **	1.7 ± 0.1 ***	-66.8 ± 0.4	26.7%	5.8 ± 0.8 ***	
C cells: Normal DRG															
siRNA n.t.	34	0.0%	50.0%	100%	0.6 ± 0.02	237.3 ± 11.3	-33.5 ± 1.6	2.5 ± 0.2	33.0 ± 1.7	0.9 ± 0.2	0.9 ± 0.2	-59.1 ± 1.5	21.2%	5.4 ± 1.0	
siRNA Nav1.6	36	0.0%	66.7%	97.2%	0.6 ± 0.03	250.3 ± 8.9	-30.6 ± 1.2	2.7 ± 0.2	37.2 ± 1.1 *	0.8 ± 0.1	0.8 ± 0.1	-56.0 ± 1.3	27.8%	7.7 ± 1.1	
A cells: LID DRG POD3															
siRNA n.t.	181	34.8%	70.7%	11.6%	17.3 ± 0.6	346.9 ± 7.4	-50.8 ± 0.5	0.78 ± 0.023	19.8 ± 0.8	0.8 ± 0.1	1.3 ± 0.1	-62.7 ± 0.5	46.4%	8.1 ± 1.3	
siRNA Nav1.6	193	6.2% ***	45.8% ***	19.7% *	15.6 ± 0.5	381.0 ± 6.8 ***	-53.4 ± 0.5 ***	0.84 ± 0.027	22.9 ± 0.7 **	1.3 ± 0.1 ***	1.4 ± 0.1	-66.6 ± 0.4 ***	31.6% **	6.7 ± 0.94 *	
C cells: LID DRG POD3															
siRNA n.t.	43	0.0%	51.2%	100%	0.6 ± 0.02	251.7 ± 6.1	-30.0 ± 0.8	2.7 ± 0.1	36.9 ± 1.0	0.8 ± 0.1	0.8 ± 0.1	-56.7 ± 1.2	9.3%	5.3 ± 0.9	
siRNA Nav1.6	39	0.0%	41.7%	97.4%	0.6 ± 0.02	255.2 ± 9.7	-33.8 ± 1.3 *	2.7 ± 0.1	36.1 ± 1.3	1.0 ± 0.2	1.0 ± 0.2	-60.6 ± 1.3 *	30.6% *	4.4 ± 0.9	

* significant difference between cells injected with siRNA against Nav1.6 and nontargeting (n.t.) control siRNA (t-test or Mann-Whitney test)

SA spontaneously active

c.v. conduction velocity

AP action potential

V voltage

Vrest resting potential

LID local inflammation of the DRG

POD postoperative day

^a Cells classified as firing multiple AP had >2 AP in response to a suprathreshold depolarizing current (includes all SA cells)^b Cells were classified as having inflected action potentials if the dV/dt measurement of the falling phase was not a simple linear decline^c Cells were classified according to whether distinctive subthreshold oscillations in the range of 100 Hz were observed during SA or during suprathreshold current injection

The maximum number of AP in response to a 270 msec suprathreshold current injection

NIH-PA Author Manuscript

NIH-PA Author Manuscript

NIH-PA Author Manuscript